Hybrid theory of P-wave electron-Li^{2+} elastic scattering and photoabsorption in two-electron systems

A. K. Bhatia
Heliophysics Science Division, NASA/Goddard Space Flight Center, Greenbelt, Maryland 20771, USA
(Received 25 January 2013; published 25 April 2013)

In previous papers [Bhatia, Phys. Rev. A **85**, 052708 (2012); **86**, 032709 (2012)] electron-hydrogen and electron-He^+ P-wave scattering phase shifts were calculated using the hybrid theory. This method is extended to the singlet and triplet electron-Li^{2+} P-wave scattering in the elastic region, where the correlation functions are of Hylleraas type. The short-range and long-range correlations are included in the Schrödinger equation at the same time, by using a combination of a modified method of polarized orbitals and the optical potential formalism. Phase shifts are compared to those obtained by other methods. The present calculation requires very few correlation functions to obtain accurate results which are rigorous lower bounds to the exact phase shifts. The continuum functions obtained in this method are used to calculate photodetachment and photoionization cross sections of two-electron systems H^-, He, and Li^+. Cross sections of the metastable $^{1,3}S$ states of He, and Li^+ are also calculated. These cross sections are calculated in the elastic region and compared with previous calculations. Using these cross sections, the Maxwellian-averaged radiative-recombination rates at various electron temperatures are also calculated.

DOI: 10.1103/PhysRevA.87.042705 PACS number(s): 34.80.Bm

I. INTRODUCTION

Collision between an electron and atom or ion is a many-body problem. The incident electron perturbs the target, inducing in it electric multipole moments. Accurate results, which are always useful for comparisons with results obtained from different approaches, can be obtained for single-electron targets because the wave function for the target is known exactly. In general, no scaling is possible to infer phase shifts, resonance parameters, photoabsorption cross sections, and radiative-attachment cross sections as the nuclear charge is increased. Therefore, it becomes necessary to carry out calculations in each case.

At low incident energies, the distortion of the target produced by the incident electron is important in addition to the exchange of the electrons. One of the methods to take into account this distortion is the method of polarized orbitals [1,2] which includes the effect of polarization in the ansatz of the wave function of the target. Various other approximations have been used: Kohn-Feshbach variational method [3], Kohn variational method [4], R-matrix method [5], and the finite element method [6]. The electron-Li^{2+} phase shifts in the elastic region have been calculated using the method of polarized orbitals by Khan *et al.* [7] and by Gien [8] using the Harris-Nesbet method. The electron-H scattering [9] and electron-He^+ [10] elastic phase shifts were calculated by using a hybrid method in which both the long-range potential proportional to $-1/r^4$ and the short-range correlations via an optical potential were included in the scattering equation at the same time. In this approach, the many-body Schrödinger equation is reduced to a single-particle Schrödinger equation. The present calculation requires very few correlation functions to obtain accurate results which are rigorous lower bounds to the exact phase shifts, provided the incident electron energy is insufficient to excite the target. Then the optical potential is negative definite and therefore corresponds to an attractive potential. Now we apply this approach to calculate phase shifts for the scattering of electrons from the doubly ionized lithium atoms, Li^{2+}.

We use the continuum functions obtained in the present formalism to calculate the photodetachment of the hydrogen ion H^-, and photoionization cross sections of He and Li^+ in the ground and metastable states at various photon energies. Using these cross sections, the Maxwellian-averaged radiative-recombination rates at various electron temperatures are also calculated. We use Rydberg units: energy in Rydbergs and length in Bohr radius a_0. The phase shifts, throughout, are in radians.

II. THEORY

We briefly describe the formalism already presented in [9,10]. In order to replace the many-body Schrödinger equation with a single-body Schrödinger equation, the total spatial wave function for electron-target partial wave (denoted by L) problem is written as

$$\Psi_L(\vec{r}_1,\vec{r}_2) = \left[\frac{u(r_1)}{r_1} Y_{L0}(\hat{r}_1)\Phi^{\rm pol}(r_1,r_2) \pm (1 \leftrightarrow 2)\right] + \sum_\lambda C_\lambda \Phi_L^\lambda(\vec{r}_1,\vec{r}_2), \quad (1)$$

where $L = 1$ in this case, and C_λ are the unknown coefficients. The summation over λ is from 1 to N, the number of terms in the expansion. The $(\pm)$ above refers to singlet (upper sign) or triplet (lower sign) scattering, respectively. In order to include the polarization of the target, the effective target function can be written as

$$\Phi^{\rm pol}(\vec{r}_1,\vec{r}_2) = \phi_0(\vec{r}_2) - \frac{\chi_\beta(r_1)}{r_1^2}\frac{u_{1s\to p}(r_2)}{r_2}\frac{\cos(\theta_{12})}{\sqrt{Z\pi}}, \quad (2)$$

where

$$\phi_0(\vec{r}_2) = \sqrt{\frac{Z^3}{\pi}} e^{-Zr_2}, \quad (3)$$

$$u_{1s\to p}(r_2) = e^{-Zr_2}\left(\frac{Z}{2}r_2^3 + r_2^2\right), \quad (4)$$

 ©2013 American Physical Society

and θ_{12} is the angle between $\vec{r}_1$ and $\vec{r}_2$. We have replaced the step function $\varepsilon(r_1,r_2)$ used in [2] by a smooth cutoff function $\chi_\beta(r_1)$, which is of the form

$$\chi_\beta(r_1) = (1 - e^{-\beta r_1})^n, \tag{5}$$

where $n \geqslant 3$. Now the polarization takes place whether the scattered electron is inside or outside the orbital electron. The polarization function given in Eq. (2) is valid throughout the range. This is unlike the step function $\varepsilon(r_1,r_2)$ used in [2] which ensures that the polarization takes place when the scattered electron r_1 is outside the orbital electron r_2. Furthermore, the function in Eq. (5) gives us another parameter β, which is a function of k, the incident electron momentum. This term guarantees that $\chi_\beta(r_1)/r_1^2 \to 0$ when $r_1 \to 0$ and it also contributes to the short-range correlations in addition to those obtained from the correlation function Φ_L, and therefore, is useful to optimize the results.

Beyond the terms containing $u(r_1)$ explicitly (those are the terms giving rise to the exchange approximation), the function Φ_L is the correlation function. For arbitrary L this function is most efficiently written in terms of the Euler angles [11]:

$$\Phi_L = \left[f_L^{\kappa,+1}(r_1,r_2,r_{12}) D_L^{\kappa,+1}(\theta,\phi,\psi) + f_L^{\kappa,-1}(r_1,r_2,r_{12}) D_L^{\kappa,-1}(\theta,\phi,\psi) \right]. \tag{6}$$

The $D_L^{\kappa,\varepsilon}$ functions ($\varepsilon = +1,-1$) are called *rotational harmonics* [11]. The f's above are the generalized "radial" functions, which depend on the three residual coordinates that are required (beyond the Euler angles) to define the two vectors $\mathbf{r}_1$ and $\mathbf{r}_2$. The distance between the two electrons is given by $r_{12} = |\vec{r}_1 - \vec{r}_2|$.

The radial functions $f_1^{1\pm}$ for $L = 1$ are defined as follows:

$$f_1^{1+} = \cos(\theta_{12}/2)[f(r_1,r_2,r_{12}) \pm f(r_2,r_1,r_{12})], \tag{7}$$

$$f_1^{1-} = \sin(\theta_{12}/2)[f(r_1,r_2,r_{12}) \mp f(r_2,r_1,r_{12})], \tag{8}$$

and

$$f(r_1,r_2,r_{12}) = \sum_{lmn} C_{lmn} r_1^l r_2^m r_{12}^n e^{-\gamma r_1 - \delta r_2}. \tag{9}$$

The upper sign in Eqs. (7) and (8) refers to the singlet state and the lower sign refers to the triplet state. The minimum value of l is equal to 1, while that of m and n is 0. The wave function of the scattered electron is given implicitly by

$$\int [Y_{L0}(\Omega_1)\Phi^{\rm pol}(\vec{r}_1,\vec{r}_2)(H - E)\Psi_L] d\vec{r}_2\, d\Omega_1 = 0, \tag{10}$$

where H is the Hamiltonian and E is the total energy of the electron target. We have, in Rydberg units,

$$H = -\nabla_1^2 - \nabla_2^2 - \frac{2Z}{r_1} - \frac{2Z}{r_2} + \frac{2}{r_{12}}, \tag{11}$$

$$E = k^2 - Z^2, \tag{12}$$

where k^2 is the kinetic energy of the incident electron and Z is the nuclear charge, which is three for Li^{2+}. The integrodifferential equation, obtained from Eq. (10) for the scattering function $u(r_1)$, has been given in the previous publication [9] and is not repeated here. The phase shifts are obtained from $u(r_1)$ for r_1 approaching infinity.

TABLE I. Comparison of phase shifts η (radians) for e-Li^{2+} scattering **without** correlations with those obtained by the method of polarized orbitals [7].

	^3P		^1P	
k	Present η	$\eta_{\rm PO}$ [7]	Present η	$\eta_{\rm PO}$ [7]
0.1	0.16323		−0.049083	
0.2	0.16334		−0.048990	
0.3	0.16341		−0.048934	
0.4	0.16351	0.1685	−0.048828	−0.05055
0.5	0.16369	0.1685	−0.048565	−0.05025
0.6	0.16379	0.1695	−0.048306	−0.04987
0.7	0.16382	0.1684	−0.047972	−0.04940
0.8	0.16374	0.1682	−0.047547	−0.04883
0.9	0.16399	0.1681	−0.046746	−0.04814
1.0	0.16409	0.1677	−0.045966	−0.04733
1.1	0.16399	0.1675	−0.045029	−0.04638
1.2	0.16378	0.1670	−0.043932	−0.04529
1.3	0.16345	0.1665	−0.042670	−0.04404
1.4	0.16299	0.1659	−0.041251	−0.04263
1.5	0.16237	0.1651	−0.039689	−0.04105
1.6	0.16158	0.1642	−0.037973	−0.03931

III. CALCULATIONS AND RESULTS

The phase shifts for ^3P and ^1P states, given in Table I, obtained without correlations are compared with those obtained in [7] using the method of polarized orbitals [2]. For the triplet states, the present phase shifts are lower than those obtained in [7], while for the singlet states they are higher. In the previous calculations for e-H and e-He^+, phase shifts obtained by the method of polarized orbitals were always higher compared to those obtained by the present method. The present results for e-Li^{2+} are lower bounds to the exact phase shifts, while those obtained by the method of polarized orbitals have no bounds.

The phase shifts for ^3P and ^1P states, given in Table II, obtained with correlations, are compared with those obtained in [8] by using the Harris-Nesbet method. The present phase shifts are higher than those obtained in [8]. Only ten correlation functions are required for ^1P states and only four correlation functions are required for ^3P states. In the ^3P states, the two electrons stay away from each other because of the Pauli principle and therefore correlations are less important. Moreover, the Coulomb potential dominates, making the correlations even less important in this case. The present phase shifts are, in general, higher than those obtained in [8] using the Harris-Nesbet method.

IV. PHOTOABSORPTION IN H^-, He, AND Li^+

In a previous paper [10], it was shown that the present approach for calculating the scattering functions can be used to calculate resonance parameters to a very high accuracy and the resonance parameters obtained for the Feshbach resonances in He and H^- agreed well with those obtained in the previous calculations using the Feshbach formalism. Now we use the continuum functions obtained by the present method to calculate photoabsorption cross sections. Photodetachment and photoionization cross sections are required to calculate

TABLE II. Phase shifts (radians) for e-Li^{2+} scattering various k for $N = 4$ for ^3P and 10 for ^1P states. $N = 20$ for ^1P states, $k = 1.2$–1.6.

	^3P		^1P	
k	Present	η (Gien)[a]	Present	η (Gien)[a]
0.1	0.17106		−0.042229	
0.2	0.17135		−0.041929	
0.3	0.17158		−0.041825	
0.4	0.17155		−0.041737	
0.5	0.17166	0.17176	−0.041407	−0.04317
0.6	0.17193	0.17167	−0.041017	−0.04205
0.7	0.17190	0.17155	−0.040686	−0.04201
0.8	0.17172	0.17141	−0.039782	−0.04125
0.9	0.17266	0.17124	−0.038966	−0.04036
1.0	0.17180	0.17105	−0.037977	−0.03932
1.1	0.17168	0.17082	−0.035725	−0.03813
1.2	0.17145	0.17056	−0.035220	−0.03676
1.3	0.17100	0.17026	−0.033851	−0.03521
1.4	0.17041	0.16991	−0.031925	−0.03345
1.5	0.16972	0.16951	−0.029898	−0.03146
1.6	0.16879	0.16906	−0.027414	−0.02923

[a]Reference [8].

radiative-attachment cross sections. The photoionization and recombination rates are needed to compute the ionization balance in astrophysical plasmas. They are also useful to probe the electron interactions with the atomic structure, and to study reactions in upper atmosphere and planetary nebulae. Atomic helium is of interest due to its high relative abundance in astrophysical plasmas. Bound-free transitions or photodetachment of H^- are required to account for the continuous absorption in the solar atmosphere. The departures of the continuous of the solar spectrum from the blackbody curves were first ascribed by Wildt [12] to the continuous absorption of radiation in H^- ions in the sun. The opacity in the sun is due to the photodetachment and free-free absorption of the radiation:

$$h\nu + \mathrm{H}^- \rightarrow \mathrm{H} + e, \tag{13}$$

$$h\nu + e + \mathrm{H} \rightarrow e + \mathrm{H}. \tag{14}$$

In the first process, the bound electron in the initial state absorbs the radiation and becomes a free electron in the final state, while in the free-free transition, the electron in the continuum state absorbs the radiation and the electron in the final state is again in a continuum state. This is the inverse process of bremsstrahlung of an electron in the vicinity of hydrogen atoms. This process was investigated by Chandrasekhar and Breen [13]. The photodetachment of H^- ions by Ar-ion laser has been used to simulate the effects of thermal and superthermal ground states of hydrogen atoms on dust grains [14].

The photodetachment or photoionization cross section (in length form and in units of a_0^2) for a transition from an initial state i to the final state f are given by

$$\sigma = 4\pi\alpha k\omega |\langle \Psi_f | z_1 + z_2 | \Phi_i \rangle|^2, \tag{15}$$

where α is the fine-structure constant, k is the momentum of the outgoing electron, and ω is the energy of the incident photon:

$$\omega = I + k^2, \tag{16}$$

where I is the ionization potential of the system absorbing the photon, and k^2 is the energy of the ejected electron, and they are in Rydberg units. We use here the length form for the cross section because this form is most suitable when the long-range correlations are included in the final-state wave function and most of the contribution to the matrix element in Eq. (15) comes from outer regions rather than the region close to the nucleus. Φ_i, the ground-state wave function of the (^1S) state as well as for metastable states (^1S and ^3S) of the two-electron system, is of the Hylleraas form and is given by

$$\Phi_i = \frac{1}{\sqrt{8\pi^2}} \sum_{lmn}^{N_\omega} C_{lmn} \left[e^{-ar_1 - br_2} r_1^l r_2^m \pm (1 \leftrightarrow 2) \right] r_{12}^n. \tag{17}$$

The upper sign refers to the singlet states and the lower sign refers to the triplet states. The nonlinear parameters a and b, and energies for a various number of terms are given in Table XI in the Appendix for H^-, He, and Li^+. The final-state wave function Ψ_f is given by Eq. (1). The expression for the cross section in Eq. (15) is obtained under the assumption that

$$u(r) \propto 1/k \quad \text{for } r \rightarrow \infty. \tag{18}$$

In Table III, we give the photodetachment of H^-, calculated without the correlation functions in Eq. (1). The cross sections have been calculated for 220, 286, and 364 terms in the bound-state wave function given in Eq. (17). Except at very low energy of the outgoing electron, the cross sections have converged in the third decimal place. The photodetachment cross section

TABLE III. Photodetachment cross sections (Mb) for the ground state of H^- without correlations and comparison with those obtained by Bell and Kingston. Momentum of the out electron is k.

k	$N_\omega = 220$	286	364	Ref. [15]
0.01	0.0243	0.0244	0.0245	
0.02	0.1914	0.1927	0.1959	
0.03	0.6306	0.6345	0.6444	
0.04	1.4449	1.4530	1.4736	
0.05	2.7015	2.7148	2.7480	
0.06	4.4275	4.4462	4.4914	
0.07	6.6082	6.6310	6.6844	
0.1	15.2147	15.2324	15.2465	12.34
0.2	38.3763	38.3675	38.3688	40.48
0.23	39.3755	39.3917	39.4354	
0.24	39.2152	39.2359	39.2882	
0.25	38.8565	38.8790	38.9121	
0.26	38.3294	38.3510	38.3850	
0.3	34.9783	34.9806	34.9684	36.40
0.4	24.2498	24.2472	24.2537	25.296
0.5	15.8663	15.8699	15.8692	16.43
0.6	10.4972	10.4942	10.4924	11.29
0.7	7.1234	7.1243	7.1258	
0.74	6.1508	6.1521	6.1530	
0.8	4.9762	4.9769	4.9768	5.31
0.8544	4.1423	4.1425	4.1421	
0.8631	4.0230	4.0228	4.0224	
0.8660	3.9852	3.9851	3.9846	

TABLE IV. Photodetachment cross sections (Mb) of the ground state of H^-. The outgoing electron has momentum k. The short-range correlations are included in the final state. N_ω is the number of terms in the bound-state function given in Eq. (17).

k	$N_\omega = 220$	286	364	PHQ[a]	Ref. [25]
0.04	1.4464	1.4545	1.4750		
0.05	2.7050	2.7185	2.7517		
0.06	4.4347	4.4534	4.4988		
0.1	15.2526	15.2704	15.3024	15.400	15.937
0.2	38.5516	38.5429	38.5443	39.411	37.870
0.23	39.5764	39.5927	39.6366		38.707
0.25	39.0699	39.0925	39.1350		38.116
0.3	35.2420	35.2443	35.2318	36.639	34.239
0.4	24.4734	24.4709	24.4774	25.296	23.858
0.5	16.0830	16.0866	16.0858	16.473	15.720
0.6	10.7459	10.7428	10.7410	11.601	10.431
0.7	7.4837	7.4847	7.4862	7.587	7.101
0.74	6.6050	6.6063	6.6072		6.139
0.8	5.6506	5.6514	5.6512	6.456	4.978
0.8544	4.1426	4.1425	4.1421		
0.8631	6.8980	6.8984	6.8976		
0.8660	7.6229	7.6230	7.6223		

[a]Reference [16].

approaches zero for $k \to 0$ because the normalized scattering function behaves like the spherical Bessel function $j_1(kr_1)$, which goes to zero for $k \to 0$. These results are compared with those of Bell and Kingston [15] who used the method of polarized orbitals. Their results are higher than the present results. This could be due to the fact that the method of polarized orbitals is not a variational one.

In Table IV, the cross sections are calculated when 35 short-range correlations are also included in the final state. The present results are compared with those obtained earlier [16] using the projection operator formalism [17], but without the polarization potential in the scattering equation. These results, though converged, are higher than the present results which include the effects of the long-range correlations as well as of the short-range correlations.

We find that at low energies the cross sections obtained by including the long-range and short-range correlations do not change significantly when compared to those obtained by including only the long-range correlations. This shows that at low energies the long-range correlations contribute the most. The two sets of cross sections are given in Fig. 1, and the deviation when k is greater than 0.6 can be seen clearly. This is due to the fact that at higher energies the electron penetrates closer to the nucleus. Beyond $k = 0.8$, the cross sections calculated by including the short-range correlations start rising because of the resonance region, which has not been investigated in this work. Therefore, the cross sections given in the figure are in the nonresonant region only.

We find that the maximum of the cross section (with or without correlations) occurs at $k = 0.23$, which corresponds to a photon of wavelength 8406.3 Å, (using $\lambda = 911.267/\omega$ Å). This agrees closely with the result obtained by Chandrasekhar [18]. There are a number of other calculations. The R-matrix results of Zhang *et al.* [19] are given only as curves and it is difficult to give a meaningful comparison with their

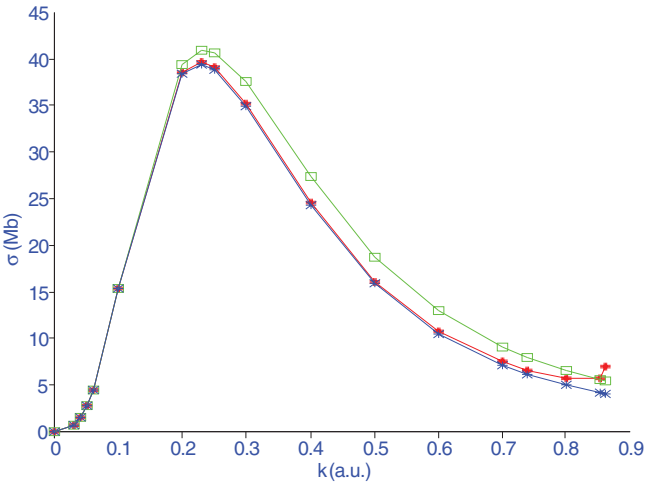

FIG. 1. (Color online) Photodetachment of a hydrogen negative ion. The lowest curve is obtained when only the long-range correlations are included; the middle curve is obtained when the short-range and long-range correlations are included. The top curve is obtained using Eq. (19).

calculations. Broad and Reinhardt [20] have carried out the calculations using the J-matrix technique. Their result at $k = 0.2$, the common point, is very close to the present results. Ohmura and Ohmura [21], using the effective range theory and the loosely bound structure of hydrogen ion, obtained

$$\sigma = \frac{6.8475 \times 10^{-18} \gamma k^3}{(1 - \gamma\rho)(\gamma^2 + k^2)^3} \text{ cm}^2, \tag{19}$$

where $\gamma = 0.235\,588\,3$, the square root of the binding energy, and $\rho = 2.646 \pm 0.004$ is the effective range. The cross sections, obtained from (19), are generally higher than the present results except at low energies where they are close to the present results. Their results are also given in Fig. 1 and the maximum in these cross sections occurs at a slightly higher incident electron momentum $k = 0.236$ or at 8195 Å.

A calculation similar to one carried out in [10], using the projection operator formalism, has also been carried out by Ajmera and Chung [22]. Their results are close to those obtained in [10], given again in Table IV. Their results were given in [10] and are not repeated here. A close-coupling calculation using pseudostates, similar to those carried out by Norcross [23] and Jacobs [24] for the metastable states in He, has been carried out by Wishart [25]. A fitting formula, given below, to these results has been obtained by Chuzhoy *et al.* [26]:

$$\sigma(\varepsilon) = \frac{2.1 \times 10^{-16} (\varepsilon - 0.75)^{1.5}}{\varepsilon^{3.11}} \text{ cm}^2, \tag{20}$$

where ε is the photon energy in units of eV. The cross sections obtained using this expression are also given in Table IV for the incident momentum $k = 0.1$–0.8. These cross sections are in good agreement with the present results. However, they are slightly lower than the present results, except at $k = 0.1$–0.4. The present calculations are expected to be fairly accurate because they include the essential physics of the problem by having an ansatz for the wave function which gives the exact polarizability of the target and also includes

TABLE V. Photoionization cross sections (Mb) of the ground state of He with outgoing electron having momentum k, without correlations in the scattering state. N_ω is the number of terms in the bound-state function given in Eq. (17).

k	$N_\omega = 120$	165	220	Ref. [30][a]
0.1	7.2634	7.2627	7.2621	7.560
0.2	7.0902	7.0888	7.0883	7.386
0.3	6.8111	6.8098	6.8094	7.083
0.4	6.4396	6.4384	6.4382	6.685
0.5	5.9948	5.9938	5.9938	6.220
0.6	5.4996	5.4989	5.4990	5.713
0.7	4.9752	4.9750	4.9751	5.185
0.8	4.4466	4.4466	4.4467	4.651
0.9	3.9294	3.9295	3.9296	4.127
1.0	3.4426	3.4428	3.4428	3.614
1.1	2.9919	2.9920	2.9920	3.152
1.2	2.5833	2.5834	2.5834	2.712
1.3	2.2191	2.2192	2.2191	2.335
1.4	1.8991	1.8991	1.8991	2.002
1.5	1.6200	1.6200	1.6200	
1.6	1.3783	1.3783	1.3783	
1.7	1.1728	1.1729	1.1729	
1.8	0.9960	0.9960	0.9960	
1.9	0.8455	0.8455	0.8455	
2.0	0.7215	0.7215	0.7215	

[a]Interpolated.

the short-range correlations. Furthermore, the calculations are variational, which results in phase shifts which have lower bounds to the exact phase shifts. In the present approach, there is no need to include pseudostates to obtain the exact polarizability of the target.

Miyska *et al.* [27] have obtained accurate results for the photodetachment of H^- using the R-matrix approach. A comparison of the present results in the nonresonant region with the R-matrix results given in Fig. 1 of [27] shows very good agreement between the two calculations. Even the shape of the present curve agrees with that of Fig. 1 [27], when plotted against the photon energy. A more definite comparison would have been possible if numerical results had been provided in addition to Fig. 1 [27].

There are experimental results [28,29] for photodetachment, given in the form of curves, and again it is not possible to make an accurate comparison with the present results. However, they appear to be close to the present results and the maximum in [28] is around 8000 Å. This is close to the calculated value, considering the resolution in the experiment is approximately 300 Å.

In Table V, the photoionization cross sections of He obtained without the short-range correlations are given for various momenta of the outgoing electron. They are given for 120, 165, and 220 terms in the ground-state wave function of the He atom. The cross sections have converged in the fourth decimal place in this case. They are compared to those obtained by Bell and Kingston [30] using the method of polarized orbitals. The cross section has a finite value for $k \to 0$, which is due to the fact the final-state wave function is a Coulomb function and $u(r) \propto 1/\sqrt{k}$, and the expression for the cross sections become independent of k, the outgoing electron momentum.

In Table VI, the cross sections are obtained by including 20 short-range correlations in the wave function for scattering. They have converged to the third decimal place. The agreement between the present results obtained using 220-term bound-state functions with the R-matrix results [31] is very good. If plotted, they can hardly be distinguished from each other. The present results are also compared with those obtained by Burke and McVicar [32] using the close-coupling approximation and the experimental results of West and Marr [33]. The experimental results, which have an accuracy of 3%, are lower than the calculated ones for $k = 0.1$–0.3, the same at $k = 0.4$, and then they are higher for $k = 0.5$–1.6. The experimental results of Samson *et al.* [34] have an accuracy of 0.1% and

TABLE VI. Photoionization cross sections (Mb) for the ground state of He obtained with correlations. The outgoing electron has momentum k.

k	$N_\omega = 120$	165	220	R matrix[a]	Ref. [32][b]	Ref. [33][b]	Ref. [34][b]
0.1	7.3319	7.3305	7.3300	7.295		7.51	7.44
0.2	7.1563	7.1549	7.1544	7.115		7.28	7.13
0.3	6.8733	6.8720	6.8716	6.838		6.93	6.83
0.4	6.4965	6.4953	6.4951	6.474		6.49	6.46
0.5	6.0471	6.0461	6.0461	6.006	5.598	5.99	6.02
0.6	5.5929	5.5924	5.5925	5.535	5.449	5.46	5.55
0.7	5.0121	5.0118	5.0120	4.985	5.103	4.92	5.04
0.8	4.4738	4.4738	4.4740	4.482	4.570	4.38	4.51
0.9	3.9647	3.9648	3.9649				
1.0	3.4652	3.4654	3.4654	3.476	3.511	3.38	3.48
1.1	3.0205	3.0206	3.0206	3.023	3.021	2.93	3.00
1.3	2.2560	2.2561	2.2561	2.271	2.293	2.17	2.19
1.4	1.9820	1.9821	1.9821	1.943	2.010	1.87	1.89
1.5	1.6816	1.6817	1.6817				
1.6	1.6324	1.6329	1.6329				

[a]Reference [31].
[b]Interpolated.

TABLE VII. Photoionization cross sections (Mb) for the ground state of Li^+ obtained with correlations. The outgoing electron has momentum k.

k	$N_\omega = 84$	120	165	Ref. [35][a]	Ref. [36][a]
0.2	2.5684	2.5679	2.5677	2.569	2.501
0.3	2.5237	2.5233	2.5231	2.520	2.432
0.4	2.4379	2.4375	2.4373	2.457	2.355
0.5	2.3875	2.3872	2.3870	2.384	2.271
0.6	2.2992	2.2989	2.2988	2.993	2.182
0.7	2.2008	2.2006	2.0005	2.206	2.087
0.8	2.0926	2.0925	2.0925	2.105	1.988
0.9	1.9792	1.9792	1.9792	1.998	1.885
1.0	1.8612	1.8612	1.8613	1.886	1.780
1.1	1.7395	1.7396	1.7396	1.770	1.674
1.2	1.6218	1.6219	1.6219	1.652	1.566
1.3	1.5033	1.5034	1.5035	1.533	1.459
1.4	1.3877	1.3878	1.3879	1.414	1.353
1.5	1.2766	1.2767	1.2768	1.297	1.248
1.6	1.1704	1.1706	1.1706	1.183	1.146

[a]Interpolated.

they are also given in Table VI. The agreement between the present results and the experimental results is fairly good.

The photoionization of positive ions is common in stellar environment. In Table VII, the photoionization cross sections of Li^+, calculated by including the long-range and short-range correlations, are given. The present results are compared with those obtained by Bell and Kingston [35] using the method of polarized orbitals. In their calculations, $\Phi^{\rm pol}$ terms were not included in the calculations of the cross sections. Daskhan and Ghosh [36] repeated these calculations by including these terms, and their results, which are lower than those of [35], are also given in the table. We have used $(2\pi a_0)^2/\alpha = 8.062$ Mb, while it is 8.067 Mb in [35] and 8.078 Mb in [36]. Their results, given in Table VII, have been corrected by using the present value, 8.062 Mb.

Photoionization of metastable states can be a significant mechanism for depopulating such states in the interplanetary nebulae. Cross sections of the $(1s2s)^{1,3}S$ states of He and Li^+, leaving the target in the $(1s)^2S$ state, are calculated using the presently calculated continuum functions for the singlet and triplet P states and they are given in Table VIII. The present results are compared with those of Norcross [23] who used the method of coupled equations for calculating the scattering functions. The present results are also compared with those of Jacobs [24] who used pseudostates $(2\bar{s},2\bar{p})$ in the coupled equations for calculating the continuum functions. His results are closer to the present results.

V. RADIATIVE ATTACHMENT

The radiative attachment plays an important role in the solar and astrophysical problems. The molecular formation takes place through such processes:

$$e + \mathrm{H} \rightarrow \mathrm{H}^- + h\nu, \tag{21}$$

$$\mathrm{H}^- + \mathrm{H} \rightarrow \mathrm{H}_2 + e. \tag{22}$$

TABLE VIII. Photoionization cross sections (Mb) for the metastable states of He and Li^+ with outgoing electron with momentum k.

			$(1s2s)\ ^1S$ state of He		
k	$N_\omega = 220$	364	455	Ref. [23][a]	Ref. [24][a]
0.1	8.7281	8.7652	8.7724	8.973	
0.2	7.5454	7.4972	7.5894	7.344	
0.3	6.0386	6.0563	6.0523	5.885	
0.4	4.5541	4.5424	4.5403	4.595	
0.5	3.2880	3.2752	3.2766	3.467	3.260
0.6	2.2116	2.2119	2.2123	2.515	2.357
0.7	1.6003	1.6052	1.6047	1.725	1.661
0.8	1.1216	1.1234	1.1230	1.104	1.141
0.9	0.7871	0.7862	0.7863	0.647	0.771
1.0	0.5483	0.5473	0.5474	0.360	0.521
1.1	0.3800	0.3796	0.3796	0.240	0.364
1.3	0.1857	0.1858	0.1858		0.212
1.4	0.1278	0.1279	0.1279		0.162
1.5	0.06998	0.07002	0.07001		0.090
			$(1s2s)\ ^3S$ state of He		
k	$N_\omega = 220$	286	364		
0.1	5.2600	5.2633	5.2629	4.749	
0.2	5.0773	5.0798	5.0795	4.564	
0.3	4.2004	4.2004	4.2004	4.112	
0.4	3.4430	3.4418	3.4403	3.537	
0.5	2.7194	2.1719	2.7189	2.912	
0.6	2.1527	2.1532	2.1531	2.295	
0.7	1.4561	1.4565	1.4564	1.733	
0.8	1.3540	1.3539	1.3539	1.256	
0.9	0.8729	0.8727	0.8728	0.885	
1.0	0.6552	0.6551	0.6551	0.623	
1.1	0.5577	0.5577	0.5577	0.463	
1.2	0.3743	0.3744	0.3744	0.383	
1.3	0.2898	0.2898	0.2898	0.347	
1.5	0.2218	0.2218	0.2218		
			$(1s2s)\ ^1S$ state of Li^+		
k	$N_\omega = 56$	84	120		
0.1	2.4241	2.4228	2.4225		
0.2	2.2312	2.3749	2.3742		
0.3	2.2247	2.2298	2.2287		
			$(1s2s)\ ^3S$ state of Li^+		
k	$N_\omega = 120$	165	220		
0.1	2.9795	3.0071	2.9889		
0.2	2.8444	2.8722	2.8570		
0.3	2.6274	2.6533	2.6434		
0.4	2.3559	2.3764	2.3733		
0.5	2.0712	2.0832	2.0865		
0.6	1.7864	1.7894	1.7962		
0.7	1.5153	1.5115	1.5182		
0.8	1.2699	1.2627	1.2627		
0.9	1.0520	1.0449	1.0462		
1.0	0.8619	0.8569	0.8560		
1.1	0.7046	0.7022	0.7003		
1.2	0.5713	0.5710	0.5693		
1.3	0.4609	0.4619	0.4607		
1.4	0.3711	0.3725	0.3721		
1.5	0.3006	0.3020	0.3020		
1.6	0.2413	0.2424	0.2427		

[a]Interpolated.

Such recombination processes took place in the early Universe when the temperature of matter and radiation came down close to a few thousand degrees. In Eq. (21), H can be replaced by He^+ and Li^{2+} to give a He atom and Li^+ ion in the final state. These processes are exothermal processes and have a small radiative-attachment cross section compared to the photodetachment or photoionization cross sections σ. The attachment cross section σ_a is given by

$$\sigma_a = \left(\frac{h\nu}{cp_e}\right)^2 \frac{g(f)}{g(i)}\sigma = \left(\frac{h\nu}{c}\right)^2 \frac{1}{2mE}\frac{g(f)}{g(i)}\sigma, \qquad (23)$$

which follows from the principle of detailed balance. In the above equation, $p_e \equiv k$ is the electron momentum. The attachment cross sections are much smaller than the photoabsorption cross sections. The radiative **r**ate coefficient averaged over the Maxwellian velocity distribution $f(E)$ is given by

$$\alpha_R(T) = \langle \sigma_a v_e f(E) \rangle , \qquad (24)$$

where v_e is the electron velocity, and the rate is given by

$$\alpha_R(T) = \sqrt{2/\pi}\frac{c}{(mc^2 k_B T)^{1.5}}\frac{g(f)}{g(i)} \times \int_0^\infty dE(E+I)^2 \sigma e^{-E/k_B T}, \qquad (25)$$

where $E = k^2$ is the energy of the electron in Eq. (21), k_B is the Boltzmann constant, T is the electron temperature, and we have used $h\nu = E + I$, where I is the threshold for photodetachment or photoionization. Considering the spin states of the electron, the angular momentum, and the polarization directions of the electromagnetic field, we find $g(i) = 12$, the statistical weight of the initial state, and $g(f) = 6(2S+1)$, the statistical weight of the final state where S is the spin of the final state of the recombined ion. The above equation has units of cm^3/s and can be written as

$$\alpha_R(T) = \frac{(2S+1)10.2509 \times 10^{10}}{(T)^{1.5}} \times \int_0^\infty dE(E+I)^2 \sigma e^{-E/k_B T}. \qquad (26)$$

TABLE IX. Recombination rate coefficients (cm^3/s) for $(1s1s)$ ^1S states of H^-, He, and Li^+.

T	$\alpha_R(T) \times 10^{15}$, H^-	$\alpha_R(T) \times 10^{13}$, He	$\alpha_R(T) \times 10^{13}$, Li^+
1000	0.99	2.50	0.12
2000	1.28	2.39	1.04
5000	2.40	1.87	2.62
7000	2.82	1.66	2.92
10000	3.20	1.45	3.03
12000	3.37	1.35	3.02
15000	3.56	1.23	2.95
17000	3.65	1.17	2.89
20000	3.75	1.10	2.79
22000	3.79	1.05	2.73
25000	3.83	0.99	2.63
30000	3.83	0.92	2.49
35000	3.77	0.87	2.36
40000	3.67	0.82	2.25

TABLE X. Recombination rate coefficients (cm^3/s) of metastable states $(1s2s)$ ^3S,^1S states of He and Li^+.

	He		Li^+	
T	$(1s2s)^3S$ $\alpha_R(T) \times 10^{14}$	$(1s2s)^1S$ $\alpha_R(T) \times 10^{15}$	$(1s2s)^3S$ $\alpha_R(T) \times 10^{14}$	$(1s2s)^1S$ $\alpha_R(T) \times 10^{14}$
1000	2.13	8.27	4.68	2.99
2000	2.08	7.97	4.47	2.87
5000	1.71	7.30	3.48	2.27
7000	1.56	5.71	3.09	2.03
10000	1.40	5.05	2.68	1.78
12000	1.32	4.73	2.49	1.66
15000	1.23	4.35	2.26	1.52
17000	1.18	4.15	2.14	1.45
20000	1.12	3.90	1.98	1.36
22000	1.09	3.75	1.90	1.31
25000	1.04	3.57	1.79	1.24
30000	0.98	3.31	1.64	1.15
35000	0.93	3.10	1.52	1.08
40000	0.89	2.93	3.143	1.02

The photoionization cross section σ in Eq. (26) is in units of Mb. The rate coefficients, Table IX, for H, He^+, and Li^{2+} have been calculated using the cross sections given in Tables IV, VI, and VII. Most of the contribution to the integrals is from the first few energy points. The present results are based on accurate photodetachment and photoionization cross sections, and therefore should be fairly accurate. They increase as the electron temperature increases, attain a maximum value, and then decrease with the increase of the temperature. The radiative rate coefficients for attachment to metastable states $(1s2s)$ $^{3,1}S$ states of He and Li^+ are given in Table X.

VI. CONCLUSIONS

We have applied the hybrid theory, in the presence of the optical potential, in which the long-range and short-range correlations have been taken into account at the same time. The present results have been calculated variationally and therefore have lower bounds to the exact phase shifts. Very few correlation terms are required to obtain accurate phase shifts. The present approach is applied to calculate photodetachment cross sections of the negative hydrogen ion and photoionization cross sections of the He atom and of the Li positive ion. The present results are in good agreement with the previous results. The photoionization cross section of He agrees very well with those obtained from R-matrix calculations. It is not possible to infer any scaling of these cross sections with the nuclear charge Z. These cross sections are used to calculate the Maxwellian-averaged radiative-attachment cross sections at various electron temperatures, the recombined states being H^-, He, and Li^+.

As for accuracy of the calculations, all phase shifts and cross sections are converged to better than the third decimal place. Perhaps the present approach, which includes the long-range and short-range correlations, will be extended to more complicated systems.

TABLE XI. Ground and excited state energies of H^-, He, and Li^+ for a various number of terms.

System	State	a	b	N_ω	E (Ry)
H^-	$(1s1s)\ ^1S$	1.27	0.58	165	−1.05550175
		1.27	0.58	220	−1.05550191
		1.27	0.58	286	−1.05550200
		1.27	0.58	364	−1.05550200
He	$(1s1s)^1S$	1.71	3.08	84	−5.80744477
		3.17	2.01	120	−5.80744840
		3.17	2.01	165	−5.80744866
		3.22	2.17	220	−5.80744872
He	$(1s2s)^3S$	2.10	0.95	165	−4.35045875
		2.10	0.95	220	−4.35045875
		2.10	0.95	286	−4.35045875
		2.10	0.95	364	−4.35045875
He	$(1s2s)^1S$	2.00	1.00	165	−4.29194713
		2.00	1.00	220	−4.29194762
		2.00	1.00	364	−4.29194796
		2.00	1.00	455	−4.29194802
Li	$(1s1s)^1S$	4.40	3.04	84	−14.5598257
		4.32	3.40	120	−14.5598265
		4.32	3.40	165	−14.5598267
Li	$(1s2s)^3S$	1.78	2.16	56	−10.2214544
		1.78	2.16	84	−10.2214547
		1.78	2.17	120	−10.2214547
Li	$(1s2s)^1S$	1.38	3.50	120	−10.0817479
		1.38	3.50	165	−10.0817509
		1.38	3.50	220	−10.0817219

TABLE XII. Comparison of the present ^1P and ^3P phase shifts (radians) for electron-hydrogen scattering with those obtained by Sloan using the method polarized orbitals.

	^1P		^3P	
k	Present η	η_{PO}	Present η	η_{PO}
0.1	0.006091	0.0067	0.009834	0.0109
0.2	0.013545	0.0171	0.041470	0.0486
0.3	0.011028	0.0210	0.095360	0.1151
0.4	0.003160	0.0163	0.164279[a]	0.2005
0.5	−0.011738	0.0064	0.234784	0.2867
0.6	−0.026733	−0.0039	0.294633	0.3574
0.7	−0.037740	−0.0100	0.33820	0.4063

[a]The phase shift for $k = 0.4$ in [9] should have been 0.148 instead of 0.0148.

ACKNOWLEDGMENT

Calculations were carried out in quadruple precision using the Discover computer of the NASA Center for Computation Science.

APPENDIX

In Table XI, we give the nonlinear parameters and ground-state energies of the H^- ion and He and Li^+ atoms for a various number of terms in the Hylleraas function, Eq. (15).

In [9], electron-hydrogen phase shifts were given using the cutoff function of Shertzer and Temkin [37]. Improved phase shifts are obtained when the cutoff given in Eq. (5) is used. The present phase shifts are given in Table XII.

[1] A. Temkin, Phys. Rev. **107**, 1004 (1957).
[2] A. Temkin and J. C. Lamkin, Phys. Rev. **121**, 788 (1961).
[3] E. McGreevy and A. L. Stewart, J. Phys. B **10**, L527 (1977).
[4] D. H. Oza, Phys. Rev. A **33**, 824 (1986).
[5] T. Scholz, P. Scott, and P. G. Burke, J. Phys. B **21**, L139 (1988).
[6] J. Botero and J. Shertzer, Phys. Rev. A **46**, R1155 (1992).
[7] P. Khan, M. Daskhan, A. S. Gosh, and C. Falcon, Phys. Rev. **26**, 1401 (1982).
[8] T. T. Gien, J. Phys. B **36**, 2291 (2003).
[9] A. K. Bhatia, Phys. Rev. A **85**, 052708 (2012).
[10] A. K. Bhatia, Phys. Rev. A **86**, 032709 (2012).
[11] A. K. Bhatia and A. Temkin, Rev. Mod. Phys. **36**, 1050 (1964).
[12] R. Wildt, Astrophys. J. **89**, 295 (1939).
[13] S. Chandrasekhar and F. H. Breen, Astrophys. J. **104**, 430 (1946).
[14] A. Chutjian, J. Simcie, S. M. Madzunkov, J. A. MacAskill, R. J. Mawhorter, and E. Tsikata, J. Phys.: Conf. Ser. **388**, 012042 (2012).
[15] K. L. Bell and A. E. Kingston, Proc. Phys. Soc. London **90**, 895 (1967).
[16] A. K. Bhatia, Phys. Rev. A **69**, 032714 (2004).
[17] H. Feshbach, Ann. Phys. (NY) **19**, 287 (1962).
[18] S. Chandrasekhar, Astrophys. J. **102**, 223 (1945).
[19] S. B. Zhang, J. G. Wang, R. K. Janev, Y. Z. Qu, and X. J. Chen, Phys. Rev. A **81**, 065402 (2010).
[20] J. T. Broad and W. P. Reinhardt, Phys. Rev. A **14**, 2159 (1976).
[21] T. Ohmura and H. Ohmura, Phys. Rev. **118**, 154 (1960).
[22] M. P. Ajmera and K. T. Chung, Phys. Rev. A **12**, 475 (1975).
[23] D. W. Norcross, J. Phys. B **4**, 652 (1971).
[24] V. Jacobs, Phys. Rev. A **3**, 289 (1971).
[25] A. W. Wishart, Mon. Not. R. Astron. Soc. **187**, 59 (1979).
[26] L. Chuzhoy, M. Kuhlen, and P. R. Shapiro, Astrophys. J. Lett. **665**, L85 (2007).
[27] S. Miyake, P. C. Stancil, H. R. Sadeghpour, A. Dalgarno, B. M. McLaughlin, and R. C. Forrey, Astrophys. J. Lett. **709**, L168 (2010).
[28] L. M. Branscomb and S. J. Smith, Phys. Rev. **98**, 1028 (1955).
[29] S. J. Smith and D. Burch, Phys. Rev. **116**, 1125 (1959).
[30] K. L. Bell and A. E. Kingston, Proc. Phys. Soc. London **90**, 31 (1967).
[31] S. N. Nahar, in *New Quests in Stellar Astrophysics. II. The Ultraviolet Properties of Evolved Stellar Populations*, edited by M. Chavez, E. Bertone, D. Rosa-Gonzalez, and L. H. Rodriguez-Merino (Springer, New York, 2009), p. 245.

[32] P. G. Burke and D. D. McVicar, Proc. Phys. Soc. London **86**, 989 (1965).
[33] J. B. West and G. V. Marr, Proc. R. Soc. London, Ser. A **349**, 397 (1976).
[34] J. A. R. Samson, Z. X. He, L. Yin, and G. N. Haddad, J. Phys. B **27**, 887 (1994).
[35] K. L. Bell and A. E. Kingston, J. Phys. B **4**, 1308 (1971).
[36] M. Daskhan and A. S. Ghosh, Phys. Rev. A **29**, 2251 (1984).
[37] J. Shertzer and A. Temkin, Phys. Rev. A **74**, 052701 (2006).